Energy Storage upon Photochromic 6-π Photocyclization and Efficient On-Demand Heat Release with Oxidation Stimuli

Ryosuke Asato, Colin Martin, Takuya Nakashima, Jan Patrick Calupitan, Gwénaël Rapenne, Tsuyoshi Kawai

Energy Storage upon Photochromic 6-π Photocyclization and Efficient On-demand Heat Release with Oxidation Stimuli

Ryosuke Asato,[†,‡] *Colin J. Martin,*[†,‡] *Takuya Nakashima,*[†] *Jan Patrick Calupitan,*[†,‡] *Gwénaël Rapenne,*[†,‡,§] *Tsuyoshi Kawai*[†,‡*]

[†] Division of Materials Science, Graduate School of Science and Technology, Nara Institute of Science and Technology, NAIST, 8916-5 Takayama-cho, Ikoma, Nara 630-0192, Japan

[‡] International Collaborative Laboratory for Supraphotoactive Systems, NAIST-CEMES, CNRS UPR 8011, 29 rue Jeanne Marvig, F-31055 Toulouse Cedex 4, France

[§] CEMES, Université de Toulouse, CNRS, 29 rue Jeanne Marvig, F-31055 Toulouse Cedex 4, France

Corresponding Author

* Tsuyoshi Kawai, Division of Materials Science, Graduate School of Science and Technology, Nara Institute of Science and Technology, NAIST, 8916-5 Takayama-cho, Ikoma, Nara 630-0192, Japan. E-mail: tkawai@ms.naist.jp.

ABSTRACT

Photochromic molecules display reversible isomerization reactions between two isomers accompanying with exchange between heat and chemical potential. A considerable part of absorbed light energy is stored in and released from the present E-type photochromic molecules, which undergo cyclization reactions under UV light excitation and backward reactions after application of oxidative stimuli. The photochromic nature, thermal stability and cascade ring-opening reaction of the closed form isomers of eight photochromic terarylenes are studied and energy storage efficiencies at a single wavelength, η as high as 23% are experimentally demonstrated. Their efficient photochemical quantum yield for the cyclization reaction markedly contributes to the high energy storage efficiency as well as showing the capability of efficient cascade cycloreversion reactions. Spontaneous cycloreversion reactions are well-suppressed as

the forbidden nature in cycloreversion reaction giving rise to sufficient heat storage duration.

TOC GRAPHICS

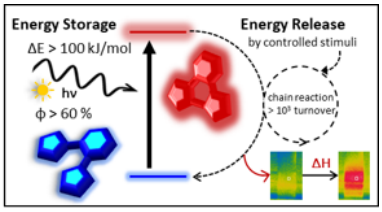

KEYWORDS

Photochromism, Molecular Solar Thermal Storage, E-type photochromic molecule, MOST, Quantum yield,

Global energy consumption has more than doubled over the past 40 years and is predicted to roughly triple by 2100 in line with growing world population.[1] The solar light hitting the earth's surface, in particular, has been widely considered as the most promising energy source. Photovoltaic silicon-based solar cells are the most widely prevailing device form with maximum theoretical efficiencies as high as 33.1%.[2] Since solar radiation is intermittent and fluctuates over time, appropriate systems for energy conversion, storage and release are desirable such as secondary batteries.[3-5] The solar

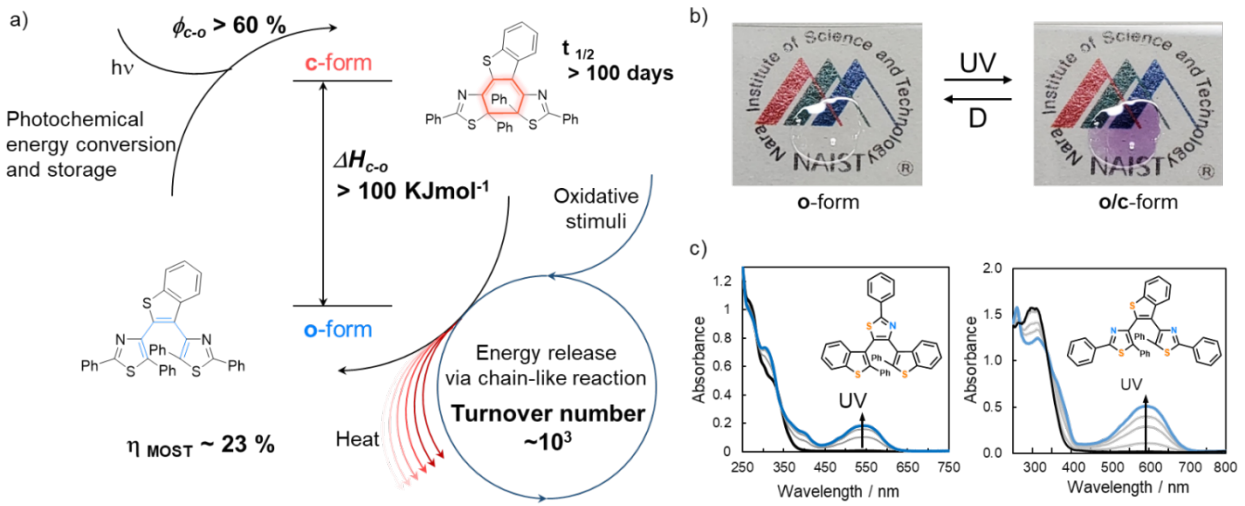

energy may also be stored and released upon the formation and dissociation of chemical bonding (e.g., as H-H, C-H and C-C bonds), as typically represented by photosynthesis.[6-10]

Figure 1. (a) Schematic diagram of MOST system based on the E-type photochromic terarylenes. The light energy is stored as the enthalpy change ($\Delta H_{c\text{-}o}$) upon photocyclization. The external oxidative stimuli trigger the intermolecular cascade reactions, leading to release of the stored energy as heat. (b) photochromic reaction of newly synthesized compound **2** in the bulk-amorphous state. (c) The UV-vis spectral changes with UV-light irradiation (365 nm) for newly synthesized compounds **2** (left) and **4** (right) in acetonitrile.

In artificial photosynthetic systems, solar energy is used to produce valuable chemicals and fuels such as methane, hydrogen and so on, through photochemical and photoelectrochemical reactions, allowing energy release in various forms such as heat through combustion.[6-10] Molecular-based energy cycles employing photoisomerization reactions have been attracting attention as solar thermal fuels which can convert, store, and release solar energy as heat. They operate in the closed systems.[11] Photochromic molecules display reversible photoisomerization reactions between thermodynamically stable and metastable isomers with color change. The photonic energy is initially converted into electronic-excitation energy followed by relaxation into a metastable isomer. Despite major part of the excitation energy being released to the surroundings as

heat, a considerable portion can be stored as the excess enthalpy of the metastable isomer.[12-25] This enthalpy can be used for heating surroundings upon the reverse isomerization reaction. Capability of on-demand heat release is thus critically desired for the **MO**lecular **S**olar **T**hermal storage (MOST) systems.[16-17]

The energy storage efficiency, η, in a MOST system is defined as the ratio of energy released upon usage (E_{out}) against the initial input energy (E_{light}) calculated over the entire solar spectrum.[18] Restricting analysis to the maximum wavelength absorption of one state of a photoswitch[19] allows for estimation of the molecules light-to-chemical-energy efficiency in terms of the wavelength at which it is absorbing. The design of photoresponsive molecules can be used to tune their efficiency through two main factors. One is the quantum yield of photoconversion reaction (ϕ) related to the efficient use of photon energy. The other is the enthalpy difference between the photoisomers (ΔH_{iso}), which roughly corresponds to the amount of released energy (E_{out}). A number of photoresponsive molecules have previously been considered as active materials in MOST systems, such as azobenzene,[18,20-22] fulvalene-tetracarbonyl-diruthenium[23-25] and norbornadiene.[26] The norbornadiene derivatives proceed $2\pi+2\pi$ reactions and their covalent C-C bonds support relatively large heat storage capacity ΔH_{iso}. They also offer relatively large activation energy for thermal back-reaction, E_a, which is also desired for

stable energy storage. The maximum energy storage efficiency of 14% was reported for an azobenzene system through the hybridization with carbon nanotubes, wherein light in the UV range was used for the energy input.[9] Moth-Poulsen and coworkers suggested a solar energy storage efficiency higher than 10% for a MOST system studied over the entire solar spectrum.[27] It has been previously calculated that the thermodynamic limit for solar spectrum storage efficiency lies in the range of 10 to 16% depending on the storage lifetime[27] with the maximum solar efficiency calculate to lie below 13%.[28]

Since η values never exceed the value of the photochemical quantum yield, $\eta<\phi$, high photo-sensitivity is critically desired for efficient MOST materials. In this regard, photochromic diarylethene (DAE) and related substances are worth to study due to their large ϕ value in the 6π-electrocyclization, which can be close to unity at certain wavelengths.[29-31] The enthalpy difference (ΔH_{c-o}) between the two photoisomers, the open (**o**) and closed (**c**) forms, was suppressed in most DAEs by means of tuning aryl units. DAEs thus behave as "P-type photochromic molecule" and the **c**-forms is stable in the dark for more than years. Therefore, most DAEs are not promising as MOST materials.[29-31] However, the accumulated findings and recent progress in DAE derivatives encourages the authors to optimize the DAE backbone to explore efficient MOST substances.[32-40] In

the present study, the authors focus on a series of terarylene derivatives (see Figure 2), as a sister substance of DAEs with an additional central aromatic unit.

The well-known Hammond's postulate[41] implies a trade-off between E_a and ΔH_{iso}. It is thus intrinsically difficult to achieve both large energy storage capacity and high thermal stability simultaneously. As like 2π +2π reactions, the 6π cyclization and cycloreversion reactions of DAE are symmetrically forbidden at the electronic ground state, which may lead to inherently high E_a values.[30,31] The estimated lifetime of a typical **c**-form DAE is 1900 years or more,[29,42] which implies an energy storage retention of 2000 times larger than the conventional lithium ion-batteries (typical self-discharge rate >40 % per year).[16,27] Irie,[43-44] Kobatake[32] and coworkers have suggested three factors for controlling the thermal stability of the metastable **c**-forms: (i) aromatic stabilization energy (ASE) of the aryl groups,[34,37,43,45] which have been reported as thiophene > thiazole > benzothiophene;[46] (ii) electron-withdrawing substituents at the aryl groups,[37-39] and (iii) steric hindrance around the substituents at the reactive carbon atoms.[32-35] Meanwhile, the additional aromatic ring in terarylene selectively stabilizes the **o**-form and elevates ΔH_{c-o}. The lifetime of **c**-forms are ranging from seconds to years and we should carefully optimize their molecular structure.[46,47] The on-demand release of heat from MOST substance requires external stimuli, such as heating,[48-51] catalyst[52-54] and oxidation

inducing catalytic exothermal reaction.[55-56] DTEs and terarylenes undergo oxidative cycloreversion after electrochemical and chemical oxidation.[57-68] These new types of photochromic molecules display highly efficient oxidative fading reactions with chain-like amplification, boosting the overall reaction efficiency up to 100,000%.[47,70] Only 10^{-3} equivalents of electrochemical or chemical oxidative stimuli could trigger the cycloreversion reaction of the entire system. They are thus facile on-demand heat release in MOST applications (Figure 1a). The present terarylene molecules, Figure 2, further display high photochromic reactivity in the bulk-amorphous state (Figure 1b), which is also advantageous for MOST materials with high energy storage density.

Synthesis and Optical Properties.

A series of terarylene derivatives comparing a variety of combinations of aromatic units by considering previously reported frameworks substituted with varying substituents were investigated as potential candidates for MOST applications (Figure 2).

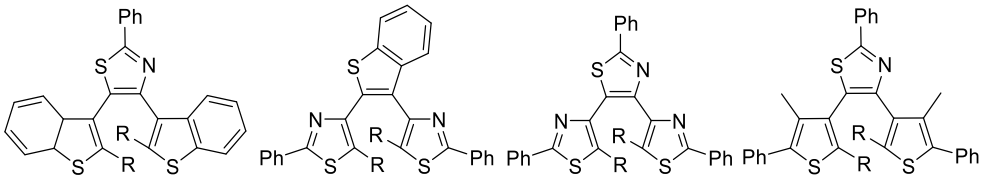

Figure 2. Molecular structures of terarylene derivatives.

Table 1. Photochemical and photothermal properties of substances.

	Photochemical properties			Photothermal properties		
	λ_{max} (**o**-form) / nm (ε/ 10^4 $M^{-1}cm^{-1}$) [a]	ϕ_{o-c} /ϕ_{c-o} [b]	$t_{1/2}$ (s) [c]	ΔH_{c-o}, DSC [i] (ΔH_{c-o},DFT[j]) / kJ mol^{-1}	Energy Density DSC (Energy Density DFT) MJ kg^{-1}	η_{DSC} (η_{DFT}) / %[k]
1	273 (2.21)	0.58/0.45[d]	4.7 x 10^7	32.7 (76.7)	0.72 (1.69)	8.2 (20)
2	249 (2.20[e])	0.57/n.a.	1.4 x 10^7	114 (136)	1.97 (2.36)	22 (26)
3	307 (2.9)	0.98/0.008[f]	1.9 x 10^8	24.8 (74.3)	0.52 (1.55)	7.7 (23)
4	303 (2.8)	0.63/n.a.	2.6 x 10^6	109.6 (129)	1.81 (2.13)	23 (27)
5	327 (3.21)	0.4/0.03 [g]	1.0 x 10^8	– (86.9)	– (1.71)	– (8.8)
6	327 (3.40)	0.12/0.03[g]	1.2 x 10^7	– (143)	– (2.26)	– (11)
7	315 (3.0)	0.6/0.07[h]	1.2 x 10^6	70.6 (98.3)	1.32 (1.84)	13 (19)
8	294 (3.12)	n.a	56	– (162)	– (2.47)	–

[a] measured in acetonitrile unless otherwise specified. ε at 350 nm in 10^4 $M^{-1}cm^{-1}$; [b] The cyclization quantum yields were estimated using an absolute photoreaction quantum yield evaluation system in toluene unless otherwise specified.[71] ; [c] measured in toluene; [d] data from ref.[72] in hexane; [e] ε was estimated at 313 nm in hexane; [f] data from ref.[73] in hexane; [g] data from ref.[70] [h] data from ref.[74] in hexane. [i] based on the integrated heat release in DSC profile and the conversion rate of **c**-form determined with UV-vis spectra; [j] data from DFT calculation with B3LYP/6-31G(d); [k] calculated using Eq. 2, at 380 nm.

All of these substances displayed reversible color change under standard terarylene conditions and concentrations upon UV and visible light irradiation,[73] and have been fully characterized in both isomers using ^{1}H-NMR and HPLC. Substances **1**,[75] **3**[73] and **7**[74] exhibited relatively high photocyclization quantum yields ($\phi_{o\text{-}c}$) over 58% as summarized in Table 1. The intramolecular non-covalent interactions between N-H, S-H and S-N atoms seems to tether them together. The rotational angle between the central and side aromatic units in the **o**-forms were selectively stabilized as the photochromic reactive "parallel" conformation. This is especially efficient in the photon-quantitative cyclization reactivity for **3** ($\phi_{o\text{-}c} \sim 98\%$).[72] Phenyl groups were then introduced at the reactive carbon atoms in **2**, **4**, **6**[70] and **8**,[76] which seems to enhance $\Delta H_{c\text{-}o}$ by elevating the enthalpy of the **c**-form due to the steric effect of the bulky substituents around the sp^3 carbon atoms. The **o**-forms showed strong absorption in the UV region below 400 nm with extinction coefficients over 10^4 $M^{-1}cm^{-1}$ at 300 nm (Table 1). The introduction of phenyl substituents on the reactive carbon atoms enhanced the extinction coefficient in the UV region (see Figure S1). All the terarylene derivatives including newly synthesized **2o** and **4o** exhibited reversible spectral changes with characteristic isosbestic points (Figure 1c, Figure S2). The introduction of phenyl rings suppressed the $\phi_{o\text{-}c}$ values and the half-lifetimes of the metastable **c**-forms. The bulky substituents at these positions were also

reported to accelerate the thermal cycloreversion reaction due to their steric effect on the **c**-form fused rings. It should be noted that the $\phi_{o\text{-}c}$ values around 0.6 for **2o** and **4o** are still more than twice those of the majority of azobenzene and norbonadiene systems. The half-lifetimes over 106 s (> 10 days) of **2c** and **4c** also appears high enough[27] for practical MOST demands. Compounds **5o** and **6o** gave relatively small $\phi_{o\text{-}c}$ values due to the preferential adoption of photochromically inactive conformations. The half-lifetime of **8c** being below 60 s is too short for full characterization and for MOST application.

These substances display color fading reactions upon addition of oxidizing reagents such as tris(4-bromophenyl)ammoniumyl hexachloroantimonate (TBPA). Specific amplified oxidative cycloreversion were observed with an amplification ratio 1:1000 or more, as like as previous substances.[47,70,76] Beside this high redox-cycloreversion capability, they showed relatively low visible light photochemical cycloreversion reactivity. **3c** for instance showed 0.8% photochemical quantum yield.[74] In this sense, **3c** may be classified not as "P-type photochromes", but as "E-type photochromes", which may be defined as molecules with photo-induced coloration isomerization and efficient reverse reaction with catalytic electro-stimulation but less-sensitive to light.

Estimation of efficiency based on Theoretical Calculations.

To achieve a large energy storage efficiency (η) a number of parameters must be optimized for photoresponsive fuel molecules. Experimentally, η may be roughly estimated on the basis of the following equation while referencing previous examples:[18]

$$\eta = \frac{E_{out}}{E_{in}} = \frac{\phi_{o-c}\Delta H_{c-o}}{E_{light\ (\lambda\ exc)} + E_{stim}} \quad (1)$$

where E_{out} and E_{in} are the output and sum of input energies respectively. The output is expressed as the product of ring-cyclization quantum yield ($\phi_{o\text{-}c}$) and the energy difference between the **o**- and **c**-forms. The input is then obtained as the sum of light radiation energy at the applied wavelength ($E_{light\ (\lambda\ exc)}$) and the energy of the external stimulus (E_{stim}) used to trigger the cycloreversion reaction for the release of stored energy (Figure 3). Since present terarylene **c**-forms exhibit efficient cascade oxidative cycloreversion[47,70,76] the E_{stim} can be small enough and we may simplify eq.(1) as,

$$\eta \approx \frac{\phi_{o-c}\Delta H_{c-o}}{E_{light\ (\lambda\ exc)}} \quad (2)$$

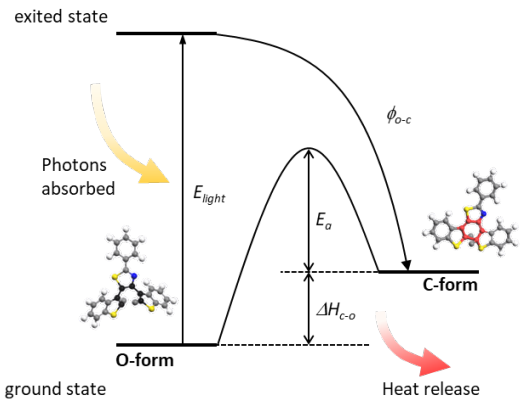

Figure 3. Energy Diagram of MOST System Based on Photochromic Terarylene.

For our estimation of storage efficiency, the photons at 380 nm (315 kJmol^{-1}) were assumed to activate the photoresponsive molecules, which is not converted in the conventional Si-based solar cells. The enthalpy differences ($\Delta H_{c\text{-}o}$) between the **o**- and **c**-forms were estimated by density functional theory (DFT) calculations using the B3LYP functional with the 6-31G(d) basis set known to give an accurate representative of terarylene energies (see Table S1 for basis set comparison).[69,77,79] Table 1 also summarizes the calculated $\Delta H_{c\text{-}o}$ for the terarylene derivatives along with their energy storage densities. Compounds **1**, **3** and **5** composed of benzo[b]thiophene and thiazole units, having less aromatic stabilization compared to thiophenes, gave smaller $\Delta H_{c\text{-}o}$ values than **7**, the system containing two thiophene rings. The introduction of phenyl groups enhances the $\Delta H_{c\text{-}o}$ value by approximately 60 kJmol^{-1} in each case. These phenyl groups are tentatively considered to selectively destabilize the **c**-forms through their steric effect on the planar fused rings. The η values under 380 nm irradiation are also estimated in Table 1. The maximum η value may be as high as 26.6 for **4o/c**. This value appears high compared to the previous norbornadiene and azobenzene substances (mostly less than 1%), however it must be considered that it is calculated only at the absorption maximum

instead of the complete solar spectrum. Indeed, previous reports show comparable efficiencies of 28% under similar single wavelength analysis.[79] We also estimated η value = 6.6 % for a typical diarylethene molecule, 4,4'-(perfluorocyclopent-1-ene-1,2-diyl)bis(5-methyl-2-phenylthiazole), based on previous experimental data and a calculated $\Delta H_{c\text{-}o}$ value. These results thus support the capability of the present molecules for MOST applications.

Study on Thermal Cycloreversion Reaction.

Arrhenius type first-order kinetics for the thermal cycloreversion reaction is of importance in the energy storage for use on a practical time scale, which is characterized by the activation barrier, E_a, from **c**- to **o**-forms (Figure 4a, Table S2 for the parameters of thermal cycloreversion reaction). Figure 4b shows the trade-off relationship between the experimentally obtained E_a and the computationally calculated $\Delta H_{c\text{-}o}$ for **1**-**8**.

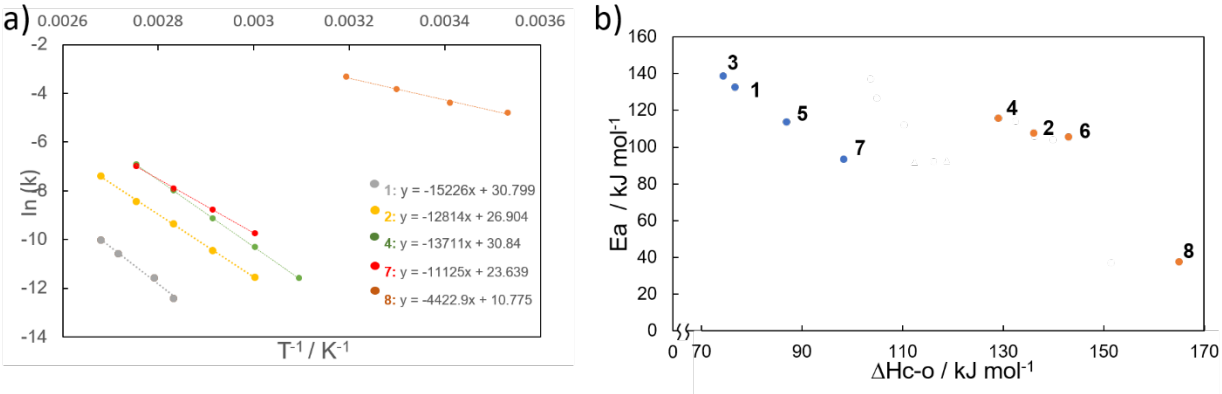

Figure 4. a) Arrhenius plots for thermal fading kinetics of terarylenes **1**, **2**, **4**, **7** and **8**; b) Activation energy E_a against ΔHc-o for compound **1**-**8**.

We may divide these substances into two classes, those with methyl groups (**1**, **3**, **5** and **7**) and those with phenyl groups (**2**, **4**, **6** and **8**) at the reaction center carbon atoms. Then, we found a linear relationship between E_a and $\Delta H_{c\text{-}o}$ values with a similar slope of about –2 for both class of substances in Figure 4b. The series of **1**, **3**, **5** and **7** share a common molecular framework of terarylene with that of **2**, **4**, **6** and **8**, respectively, and have three aromatic units involved in the 6π-photocyclization. These three aromatic rings are collapsed upon photocyclization and recovered in the cycloreversion reaction. The sum of aromatic stabilization energy of these aryl units may predominantly contribute to this E_a-$\Delta H_{c\text{-}o}$ relationship. The higher aromatic stabilization in the **o**-form may also have an effect on the transition state and suppress E_a, which supports the Hammond's postulate. The negative slope of about -2 seems to be unique for the 6π-electrocyclization reaction in the terarylene framework. This slope is frequently between 0 and -1 for most thermal reaction systems under the classic linear free energy relationship, LFER. The aromatic rings in the present systems affects twice strongly for the activation barrier than the relative stability of **o**-form. Therefore, molecular tuning of molecular design based on the

aromatic stabilization energy is strongly limited by the Hammond's postulate. Interestingly, the phenyl rings on the reactive carbon atoms did not change the slope but induced a significant parallel shift and increased $\Delta H_{c\text{-}o}$. This observed trend suggests possibly overcoming the trade-off between $\Delta H_{c\text{-}o}$ and E_a by means of introduction of substituent groups at the reaction center carbon atoms.

We can also compare our results with representative examples of diarylethene systems (Figure S2) over which they show enhanced storage properties, as well as other MOST molecules such as azobenzene[16] and norbornadiene[26,27] derivatives in term of the ΔH_{iso} and E_a relationship (Figure S2, S3). Both the photoresponsive scaffolds gave a good linear trade-off relationship in E_a-ΔH_{iso}. Among these substances, the present terarylene substances, especially those with phenyl substituents, displayed data distribution at large ΔH_{iso} with similar or little higher E_a, suggesting the favorable characteristics of terarylenes in terms of energy storage efficiency.

We then experimentally evaluated the $\Delta H_{c\text{-}o}$ value by means of differential scanning calorimetry (DSC). Compounds **1**, **2**, **3**, **4** and **7** with relatively high $\phi_{o\text{-}c}$ and reasonable thermal stability were selected. The heat release at the first heating scan of samples containing a photostationary state mixture was recorded as an exothermic peak in the DSC thermograms (Figure S4). The successive second scan gave no such exothermic

peak for all samples, suggesting the first scan peak corresponds to the heat release at the cycloreversion reaction of the **c**-form. The heat release associated with the crystalline-phase transition was not observed due to the amorphous character of these samples. The second scan profiles were thus used for correcting background heat-flow. We evaluated $\Delta H_{c\text{-}o}$ values from the peak integral and the amount of **c**-form present (Table S3). These experimentally estimated values roughly coincide to the results of DFT calculations with minor deviation because of effects of medium and intermolecular interaction. The energy storage efficiency was then evaluated from the DSC profiles as η_{DSC} values and also summarized in Table 1. The high η_{DSC} values obtained for compounds **2** and **4**, 22% and 23% respectively, seems to indicate they are particularly promising for energy storage applications.

Heat Release Triggered by Oxidation as E-type photochromes.

The release of stored energy in the terarylene-based system can also be triggered by the oxidative cycloreversion reaction, proceeding via a chain-reaction manner. The heat release is demonstrated by adding a small amount of chemical oxidant (TBPA) to an acetonitrile solution containing the **c**-form of **1** (5.0×10^{-2} mM). The surface temperature of the solution was monitored using a thermography camera. As shown in Figure 5a, after

the addition of oxidant (5 mol% eq.) the solution temperature increased by 3°C. The temperature change was also monitored using a thermocouple thermometer (Figure 5b). The addition of the oxidant induced heat release, with the temperature increasing from 27°C to 30°C. The temperature was stable at 30°C for around 10 seconds, indicating good thermal balance.

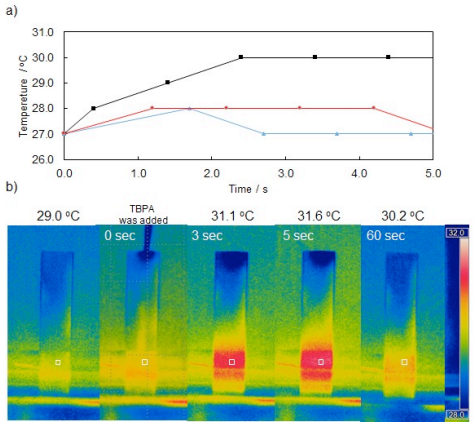

Figure 5. a) Temperature increase after adding 5 mol% of TBPA in acetonitrile (0.05 mL) into 1 mL of chloroform solution of **7c/o** (black), **7o** (red), and only chloroform (blue). Concentration of **c**-form = 5.0 x 10^{-2} M. The temperature was monitored by a sheathed thermocouple. b) Thermographic images after adding 5 mol% of TBPA in acetonitrile (0.05 mL) into chloroform (1 mL) in a quartz cell.

The ideal temperature increase was roughly calculated from the $\Delta H_{c\text{-}o}$ based on DFT, amount of **c**-form, and heat capacity of the solvent to be 2.9°C, which roughly agreed with the observed temperature change. The heating effect of initial oxidation is much smaller than the heat release by the **c**-form thanks to the cascade reaction capability which indicates the advantage of this strategy. The concentration of the solution should be increased for future practical investigation as the heat density is important for practical applications. Electrochemical oxidation stimulation may also be conventionally used in practical MOST systems, which should be a subject of future studies.

The light to chemical storage efficiency at a single illumination wavelength for eight terarylenes, including two new substances of E-type photochromic nature was investigated for MOST applications. The terarylene framework was strategically designed by considering energy difference between the photoisomers ($\Delta H_{c\text{-}o}$), which corresponds to the amount of stored (and released) energy. The $\Delta H_{c\text{-}o}$ likely stems from i) the increasing steric hindrance around the substituent groups on the reaction center carbon atoms and ii) the loss of aromatic stabilization energy upon the photoisomerization from **o**- to **c**-forms. According to the computationally estimated values of $\Delta H_{c\text{-}o}$, a framework containing benzothiophene or thiophene as the central aromatic moiety and phenyl rings as a bulky substituent at reactive carbon atoms, such as **2**, **4** or **6** are the best to enhance

$\Delta H_{c\text{-}o}$. High photo-cyclization quantum yield (ϕ_{iso}) is achieved by locking the **o**-form in its photoreactive conformation using intramolecular non-bonding interactions inherent to terarylene. These high $\Delta H_{c\text{-}o}$ and ϕ_{iso} values support maximum efficiencies at a single wavelength of 22% for **2** and 23% for **4**. These values are comparable with existing single wavelength MOST storage systems and offer a potential future framework to study such behavior under broad wavelength conditions. The well-known Hammond's postulate and the trade-off relation between the activation energy (E_a) and $\Delta H_{c\text{-}o}$ were experimentally observed in the terarylenes and some previous substances. The sum of aromatic stabilization energy of the three aryl units in the terarylene framework seems predominantly contribute to the E_a-$\Delta H_{c\text{-}o}$ relationship. We tentatively classified these terarylenes into two groups based on the distribution of E_a-$\Delta H_{c\text{-}o}$ data plots, depending on the substituent groups. The present terarylenes showed significantly large $\Delta H_{c\text{-}o}$ compared to previous substances with similar or higher E_a value. Particularly, the introduction of phenyl rings was much advantageous for enhancing $\Delta H_{c\text{-}o}$ with only a minor loss in E_a. In addition to relatively high photochemical cyclization quantum yield, the E-type photochromic nature of terarylenes with significant amplification cycloreversion behavior seems to offer an interesting potential for future MOST substances. Considering the energy capacity of the terarylene scaffold, the present highest $\Delta H_{c\text{-}o}$ is 114 $kJmol^{-1}$ for

2, which is surprisingly as high as about one-third of the photon energy at 380 nm. Terarylene is also advantageous as being highly photoreactive with excellent recyclability even in amorphous and crystalline solids, which may provide very high energy density. These excellent features of terarylenes motivate us to explore further optimization of molecular structure for future MOST applications particularly looking at expanding towards the entire solar spectrum.

ASSOCIATED CONTENT

Supporting Information. Further photophysical, thermal and characterization data, including full NMR and MS data for all new compounds, along with X-Ray crystallographic data for **4o** and DFT summaries for **1-8**. This material is available free of charge via the Internet at http://pubs.acs.org.

AUTHOR INFORMATION

Notes

The authors declare no competing financial interests.

ACKNOWLEDGMENT

This work was supported by the MEXT Program for Promoting the Enhancement of Research Universities in NAIST, the CNRS and the University Paul Sabatier (Toulouse). This research was partly supported by the JSPS KAKENHI Grant Number JP26107006 in Scientific Research on Innovative Areas “Photosynergetics”. RA thanks the NAIST foundation for financial support and CM thanks the JSPS KAKENHI Grant-in-Aid for Early-Career Scientists (19K15312).

REFERENCES

(1) BP Statistical Review of World Energy, London, BP, **2020**, bp.com/statisticalreview.

(2) Shockley, W.; Queisser, H. J. Detailed balance limit of efficiency of p-n Junction solar cells. *J. Appl. Phys.* **1961**, *32*, 510-519.

(3) Pagliaro, M.; Konstandopoulos, A. G.; Ciriminna R.; Palmisano, G. Solar hydrogen: fuel of the near future. *Energy Environ. Sci.* **2010**, *3*, 279-287.

(4) Ausfelder, F. et al. Energy Storage as Part of a Secure Energy Supply. *ChemBioEng Rev.* **2017**, *4*, 144-210.

(5) Cook, T. R. et al. Solar energy supply and storage for the legacy and nonlegacy worlds. *Chem. Rev.* **2010**, *110*, 6474-6502.

(6) Schnatbaum, L. Solar thermal power plants. *Eur. Phys. J. Spec. Top.* **2009**, *176*, 127-140.

(7) Roeb, M.; Neises, M.; Monnerie, N.; Sattler C.; Pitz-Paal, R. Technologies and trends in solar power and fuels. *Energy Environ. Sci.* **2011**, *4*, 2503-2511.

(8) Piatkowski, N.; Wieckert, C.; Weimerc W. A.; Steinfeld, A. Solar-driven gasification of carbonaceous feedstock—a review. *Energy Environ. Sci.* **2011**, *4*, 73-82.

(9) Gil, A. et al. State of the art on high temperature thermal energy storage for power generation. Part 1—Concepts, materials and modellization. *Renew. Sust. Energy Rev.* **2010**, *14*, 31-55.

(10) Coelho, B.; Oliveira C. A.; Mendes, A. Concentrated solar power for renewable electricity and hydrogen production from water-a review. *Energy Environ. Sci.* **2010**, *3*, 1398-1405.

(11) Jones II, G.; Chiang S.-H.; Xuan, T. P. Energy storage in organic photoisomers. J. *Photochem.* **1979**, *10*, 1-18.

(12) Dubonosov, D. A.; Bren V A.; Chernoivanov, V. A. Norbornadiene-quadricyclane as an abiotic system for the storage of solar energy. *Russ. Chem. Rev.* **2002**, *71*, 917-927.

(13) Taoda, H.; Hayakawa, K.; Kawase K.; Yamakita, H. J. Photochemical Conversion and Storage of Solar Energy by Azobenzene. *Chem. Eng. Jpn.* **1987**, *20*, 265–270.

(14) Pouliquen, J.; Wintgens, V.; Toscano, V.; Jaafar, B. B.; Tripathi, S.; Kossanyi, J.; Valat., P. Photoisomerization of N,N'-disubstituted indigos. A search for energy storage, *Can. J. Chem.* **1984**, *62*, 2478-2486.

(15) Olmsted, J.; Lawrence III, J.; Yee, G. G. Photochemical storage potential of azobenzenes. *Sol. Energy*. **1983**, *30*, 271-274.

(16) Kucharski, T. J.; Tian, Y.; Akbulatov, S.; Boulatov, R. Chemical solutions for the closed-cycle storage of solar energy. *Energy Environ. Sci.* **2011**, *4*, 4449-4472.

(17) Kathan, M.; Hecht, S. Photoswitchable molecules as key ingredients to drive systems away from the global thermodynamic minimum. *Chem. Soc. Rev.* **2017**, *46*, 5536-5550.

(18) Kucharski, T. et al. Templated assembly of photoswitches significantly increases the energy-storage capacity of solar thermal fuels. *Nature Chem.* **2014**, *6*, 441-447.

(19) Moormann, W.; Tellkamp, T.; Stadler, E.; Röhricht, F.; Näther, C.; Puttreddy, R.; Rissanen, K.; Gescheidt, G.; Herges R. Efficient Conversion of Light to Chemical Energy: Directional, Chiral Photoswitches with Very High Quantum Yields. *Angew. Chem. Int. Ed.* **2020**, *59*, 15081-15086.

(20) Ishiba, K. et al. Photoliquefiable ionic crystals: A phase crossover approach for photon energy storage materials with functional multiplicity. *Angew. Chem. Int. Ed.* **2014**, *54*, 1532-1536.

(21) Kolpak, A. M.; Grossman, J. C. Azobenzene-functionalized carbon nanotubes as high-energy density solar thermal fuels. *Nano Lett*. **2011**, *11*, 3156-3162.

(22) Nishimura, S.; Yamanaka, H.; Imai, E.; Yamamoto, S.; Hasegawa, S. Thermal cis-to-trans isomerization of substituted azobenzenes II. Substituent and solvent effects. *Bull. Chem. Soc. Jpn*. **1976**, *49*, 1381-1387.

(23) Kanai, Y.; Srinivasan, V.; Meier, S. K.; Vollhardt K. P. C.; Grossman, J. C. Mechanism of thermal reversal of the (fulvalene)tetracarbonyldiruthenium photoisomerization: Toward molecular solar-thermal energy storage. *Angew. Chem. Int. Ed*. **2010**, *49*, 8926-8929.

(24) Boese, R. et al. Photochemistry of (fulvalene)tetracarbonyldiruthenium and its derivatives: Efficient light energy storage devices. *J. Am. Chem. Soc*. **1997**, *119*, 6757-6773.

(25) Vollhardt, K. P. C.; Weidman, T. W. Synthesis, structure, and photochemistry of tetracarbonyl(fulvalene)diruthenium. Thermally reversible photoisomerization involving carbon-carbon bond activation at a dimetal center. *J. Am. Chem. Soc*. **1983**, *105*, 1676-1677.

(26) Petersen, A. U. et al. Solar energy storage by molecular norbornadiene-quadricyclane photoswitches: polymer film devices. *Adv. Sci*. **2019**, *6*, 1900367.

(27) Börjesson, K.; Lennartson, A.; Moth-Poulsen, K. Efficiency limit of molecular solar thermal energy collecting devices. *ACS Sustainable Chem. Eng*. **2013**, *1*, 585-590.

(28) Wang Z.; Moïse, H.; Cacciarini, M.; Brøndsted Nielsen, M.; Morikawa, M.; Kimizuka, N.; Moth-Poulsen, K. Liquid-Based Multijunction Molecular Solar Thermal Energy Collection Device. Adv. Sci. **2021**, Early view doi:10.1002/advs.202103060.

(29) Irie, M.; Mohri, M. Thermally irreversible photochromic systems. Reversible photocyclization of diarylethene derivatives. *J. Org. Chem.* **1988**, *53*, 803–808.

(30) Irie, M.; Fukaminato, T.; Matsuda, K.; Kobatake, S. Photochromism of diarylethene molecules and crystals: Memories, switches, and actuators. *Chem. Rev.* **2014**, *114*, 12174-12277.

(31) Irie, M. Diarylethenes for memories and switches. *Chem. Rev.* **2000**, *100*, 1685–1716.

(32) Kitagawa, D.; Kobatake, S. Strategy for molecular design of photochromic diarylethenes having thermal functionality. *Chem. Rec.* **2016**, *16*, 2005–2015.

(33) Morimitsu, K.; Shibata, K.; Kobatake, S.; Irie, M. Dithienylethenes with a novel photochromic performance. *J. Org. Chem.* **2002**, *67*, 4574-4578.

(34) Kobatake, S.; Uchida, K.; Tsuchida, E.; Irie, M. Photochromism of diarylethenes having isopropyl groups at the reactive carbons. Thermal cycloreversion of the closed-ring isomers. *Chem. Lett.* **2000**, *29*, 1340-1341.

(35) Morimitsu, K.; Shibata, K.; Kobatake, S.; Irie, M. Thermal cycloreversion reaction of a photochromic dithienylperfluorocyclopentene with tert-butoxy substituents at the reactive carbons. *Chem. Lett. 2002*, 31, 572-573.

(36) Chen, Z. D.; Wang, Z.; Zhang, H. H. Theoretical study on thermal stability and absorption wavelengths of closed-ring isomers of diarylethene derivatives. *J. Mol. Struct.* **2008**, 859, 11-17.

(37) Shirinian, Z. V.; Lvov, G. A.; Krayushkin, M. M.; Lubuzh, E. D.; Nabatov, B. V. Synthesis and comparative photoswitching studies of unsymmetrical 2,3-diarylcyclopent-2-en-1-ones. *J. Org. Chem.* **2014**, *79*, 3440-3451.

(38) Liu, G.; Pu, S.; Wang, R. Photochromism of asymmetrical diarylethenes with a pyrrole unit: Effects of aromatic stabilization energies of aryl rings. *Org. Lett.* **2013**, *15*, 980-983.

(39) Kobatake, S.; Irie, M. Synthesis and photochromism of diarylethenes with isopropyl groups at the reactive carbons and long π-conjugated heteroaryl groups. *Chem. Lett.* **2003**, *32*, 1078-1079.

(40) Gilat, S. L.; Kawai, S. H.; Lehn, J. M. Light-triggered molecular devices: Photochemical switching of optical and electrochemical properties in molecular wire type diarylethene species. *Chem. Eur. J.* **1995**, *1*, 275-284.

(41) Hammond, G. S. A correlation of reaction rates. *J. Am. Chem. Soc.* **1955**, 77, 334-338.

(42) Irie, M.; Lifka, T.; Kobatake, S.; Kato, N. Dithienylethenes with a novel photochromic performance. *J. Am. Chem. Soc.* **2002**, *122*, 4871-4876.

(43) Nakamura, S. et al. Theoretical investigation on photochromic diarylethene: A short review. *J. Photochem. Photobiol. A.* **2008**, *200*, 10–18.

(44) Nakamura, S.; Irie, M. Thermally irreversible photochromic systems. A theoretical study. *J. Org. Chem.* **1988**, *53*, 6136-6138.

(45) Liu, G.; Pu, S.; Wang, R. Photochromism of asymmetrical diarylethenes with a pyrrole unit: Effects of aromatic stabilization energies of aryl rings. *Org. Lett.* **2013**, *15*, 980-983.

(46) Kawai, S. et al. Novel photochromic molecules based on 4,5-dithienyl thiazole with fast thermal bleaching rate. *Chem. Mater.* **2007**, *19*, 3479-3483.

(47) Nakashima, T. et al. Efficient oxidative cycloreversion reaction of photochromic dithiazolylthiazole. *J. Am. Chem. Soc.* **2012**, *134*, 19877-19883.

(48) Bandarab, H. M. D.; Burdette, S. C. Photoisomerization in different classes of azobenzene. *Chem. Soc. Rev.* **2012**, *41*, 1809-1825.

(49) Brummel, O. et al. Energy storage in strained organic molecules: (Spectro)electrochemical characterization of norbornadiene and quadricyclane. *ChemSusChem.* **2016**, *9*, 1424-1432.

(50) Dreos, A. Exploring the potential of a hybrid device combining solar water heating and molecular solar thermal energy storage. *Energy Environ. Sci.* **2017**, *10*, 728-734.

(51) Moth-Poulsen K. et al. Molecular solar thermal (MOST) energy storage and release system. *Energy Environ. Sci.* **2012**, *5*, 8534-8537.

(52) Koser, G. F.; Faircloth, J. N. Silver(I)-promoted reactions of strained hydrocarbons. Oxidation vs. rearrangement. *J. Org. Chem.* **1976**, *41*, 583-585.

(53) Maruyama, K.; Tamiaki, H.; Kawabata, S. Development of a solar energy storage process. Photoisomerization of a norbornadiene derivative to a quadricyclane derivative in an aqueous alkaline solution. *J. Org. Chem.* **1985**, *50*, 4742-4749.

(54) Hoffmann, R. W.; Barth, W. ECE-catalysed isomerisation of quadricyclanes. *J. Chem. Soc., Chem. Commun.* **1983**, 345–346.

(55) Wang, Z., et al. Macroscopic heat release in a molecular solar thermal energy storage system. *Energy Environ. Sci.* **2019**, *12*, 187–193.

(56) Waidhas, F. et al. Electrochemically controlled energy storage in a norbornadiene-based solar fuel with 99% reversibility. *Nano Energy* **2019**, *63*, 103872.

(57) Koshido, T.; Kawai, T.; Yoshino, K. Optical and electrochemical properties of cis-1,2-dicyano-1,2-bis(2,4,5-trimethyl-3-thienyl)ethene. *J. Phys. Chem.* **1995**, *99*, 6110-6114.

(58) Moriyama, Y.; Matsuda, K.; Tanifuji, N.; Irie, S.; Irie, M. Electrochemical cyclization/cycloreversion reactions of diarylethenes. *Org. Lett.* **2005**, *7*, 3315-3318.

(59) Peters, A.; Branda, N. R. Electrochromism in photochromic dithienylcyclopentenes. J. Am. Chem. Soc. 125, 3404-3405 (2013).

(60) Browne, R. W. et al. Oxidative electrochemical switching in dithienylcyclopentenes, Part 2: Effect of substitution and asymmetry on the efficiency and direction of molecular switching and redox stability. *Chem. Eur. J.* **2005**, *11*, 6414-6429.

(61) Gorodetsky, B.; Branda, N. R. Bidirectional ring-opening and ring-closing of cationic 1,2-dithienylcyclopentene molecular switches triggered with light or electricity. *Adv. Funct. Mater.* **2007**, *17*, 786-796.

(62) Guirado, G.; Coudret, C.; Launay, J-P. Electrochemical remote control for dithienylethene-ferrocene switches. *J. Phys. Chem. C.* **2007**, *111*, 2770-2776.

(63) Staykov, A.; Areephong, J.; Browne, W. R.; Feringa, B. L.; Yoshizawa, K. Electrochemical and photochemical cyclization and cycloreversion of diarylethenes and diarylethene-capped sexithiophene wires. *ACS Nano* **2011**, *5*, 1165-1178.

(64) Lee, S.; You, Y.; Ohkubo, K.; Fukuzumi, S.; Nam, W. Highly efficient cycloreversion of photochromic dithienylethene compounds using visible light-driven photoredox catalysis. *Chem. Sci.* **2014**, *5*, 1463-1474.

(65) Lee, S.; You, Y.; Ohkubo, K.; Fukuzumi, S.; Nam, W. Photoelectrocatalysis to improve cycloreversion quantum yields of photochromic Ddthienylethene compounds. *Angew. Chem. Int. Ed.* **2012**, *51*, 13154-13158.

(66) Akita, M. Photochromic organometallics, a stimuli-responsive system: An approach to smart chemical systems. *Organometallics*. **2011**, *30*, 43-51.

(67) Mulas, A. et al. Dual-responsive molecular switches based on dithienylethene-Ru II organometallics in self-assembled monolayers operating at low voltage. *Chem. Eur. J.* **2017**, *23*, 10205-10214.

(68) Julià-López, A. et al. Temperature-controlled switchable photochromism in solid materials *Angew. Chem. Int. Ed.* **2016**, *55*, 15044-15048.

(69) Calupitan, J. P. D. C.; Nakashima, T.; Hashimoto, Y.; Kawai, T. Fast and efficient oxidative cycloreversion reaction of a π-extended photochromic terarylene. *Chem. Eur. J.* **2016**, *22*, 10002-10008.

(70) Kutsunugi, Y.; Kawai, S.; Nakashima, T.; Kawai, T. Photochromic properties of terarylene derivatives having a π-conjugation unit on central aromatic ring. *New J. Chem.* **2009**, *33*, 1368-1373.

(71) Kawai, S. et al. Photochromic amorphous molecular materials based on dibenzothienylthiazole structure. *J. Mater. Chem.* **2009**, *19*, 3606-3611.

(72) Jorner, K. et al. Unraveling factors leading to efficient norbornadiene–quadricyclane molecular solar-thermal energy storage systems. *J. Mater. Chem. A.* **2017**, *5*, 12369-12378.

(73) Nakashima, T. et al. Photochromism of thiazole-containing triangle terarylenes. *Eur. J. Org. Chem.* **2007**, 3212-3218.

(74) Asato, R. et al. Photosynergetic amplification of radiation input: from efficient UV induced cycloreversion to sensitive X-ray detection. *Chem. Sci.* **2020**, 11, 2504-2510.

(75) Fukumoto, S.; Nakashima, T.; Kawai, T. Photon-quantitative reaction of a dithiazolylarylene in solution. *Angew. Chem. Int. Ed.* **2011**, *50*, 1565-1568.

(76) Nakashima, T. et al. Self-contained photoacid generator triggered by photocyclization of triangle terarylene backbone. *J. Am. Chem. Soc.* **2015**, *137*, 7023-7026.

(77) Van Dyck, C.; Geskin, V.; Cornil, J. NEGF-DFT characterization of diarylethene photoswitches: Impact of substituents. *AIP Conference Proceedings* **2015**, *1642*, 505.

(78) Calupitan, J. P. D. C. et al. Adsorption of Terarylenes on Ag(111) and NaCl(001)/Ag(111): A Scanning Tunneling Microscopy and Density Functional Theory Study. *J. Phys. Chem. C.* **2018**, *122*, 5978–5991.

(79) Dreos, A.; Wang, Z.; Udmark, J.; Ström, A.; Erhart, P.; Börjesson, K.; Brøndsted Nielsen, M.; Moth-Poulsen. K. Liquid Norbornadiene Photoswitches for Solar Energy Storage. *Adv. Energy Mater.* **2018**, 1703401.

Supplementary Information

Ryosuke Asato,[†,‡] *Takuya Nakashima*,[†] *Colin J. Martin*,[†,‡] *Jan Patrick Calupitan*,[†,‡]

Gwénaël Rapenne,[†,‡,§] *Tsuyoshi Kawai*[†,‡*]

† Division of Materials Science, Graduate School of Science and Technology, Nara Institute of Science and Technology, NAIST, 8916-5 Takayama-cho, Ikoma, Nara 630-0192, Japan

‡ International Collaborative Laboratory for Supraphotoactive Systems, NAIST-CEMES, CNRS UPR 8011, 29 rue Jeanne Marvig, F-31055 Toulouse Cedex 4, France

§ CEMES, Université de Toulouse, CNRS, 29 rue Jeanne Marvig, F-31055 Toulouse Cedex 4, France.

Corresponding author: * tkawai@ms.naist.jp

Experimental details

General

General ^{1}H and ^{13}C NMR (300, 400 and 600 MHz) spectra were recorded on *JEOL* JNM-AL300, *JEOL* JNM-ECP400 and *JEOL* JNMECA600 spectrometers, respectively. Recycling preparative GPC were performed on *Japan Analytical Industry* LC-9110NEXT. Mass spectrometry and high-resolution mass spectrometry were performed on matrix assisted laser desorption/ionization (MALDI) time of Flight (TOF) – MS spectra (*Bruker* Autoflex II and *JEOL* spiralTOF JMS-S3000). UV/Vis spectra, quantum yields of photochromic reactions ($\phi_{c\text{-}o}$ and $\phi_{o\text{-}c}$) and photo-induced fading reaction were measured using a *JASCO* V-660, V-760 spectrophotometer and a *Shimadzu* QYM-01 set-up, respectively. Calculations were performed with the Gaussian09 package.[1] We worked at the B3LYP 6-31G(d) level of theory in vacuo. For kinetic thermal analyses, the temperature was controlled by a *JASCO* ETC 505 T temperature controller. Heat quantity was measured using Differential scanning calorimeter, *SHIMAZU* DSC-60Plus and *SHIMAZU* TA-60WS thermal analyzer. For the demonstration of heat release system, the temperature was monitored by *CHINO* sheathed thermocouple (ϕ 0.3 mm) and *Fine* FHP301Npro. Thermographic images were recorded on Optris Compact spot finder IR camera Xi 400.

General Synthesis

Compounds **1**,[68] **3**,[69] **5**,[45] **6**,[67] **7**[69] and **8**[71] were synthesized as previously reported. compound **2** and **4** were prepared according to the routes depicted in Schemes 1 and 2. Compounds **S1**,[70] **S4**,[73] **S5**[69] were prepared as previously reported, and compound **S2** was commercially available. The structures have all been successfully characterized using NMR and HR-MS. NMR and MS spectra are in the supplementary information (Figures S13-S16).

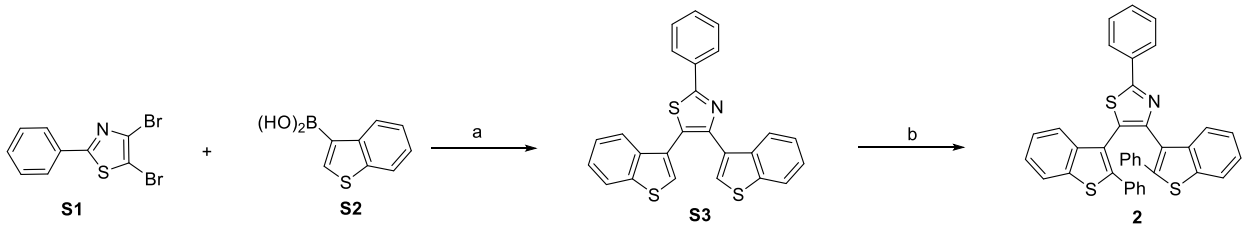

Scheme 1. *Synthesis of **2**: a) [Pd(PPh$_3$)$_4$], PPh$_3$, 2 M K$_3$PO$_4$, water/1,4-dioxane, THF, 24 h, 110 °C; b) Boronic acid, (^{t}Bu)$_2$PMeHBF$_4$, pivalic acid, Cs$_2$CO$_3$, Pd(OAc)$_2$ 16 h, 150 °C.*

4,5-bis(benzothiophen-3-yl)-2-phenylthiazole (**S3**): A two-necked flask was charged with 4,5-dibromo-2-phenylthiazole (**S1**) (0.48 g, 2.0 mmol), benzothiophen-3-ylboronic acid (**S2**) (1.28 g, 4.4 mmol), triphenylphosphine (0.26 g, 1.0 mmol) and 2 M aqueous tripotassium phosphate (15 mL) in 1,4-dioxane (15 mL). After 15 minutes of stirring under a nitrogen atmosphere, tetrakis(triphenylphosphine)palladium(0) (0.34 g, 0.2 mmol) was added and stirred under nitrogen atmosphere at 110°C for 24 hours. The

organic layer was then extracted with chloroform, and the combined extracts were washed with water and dried over anhydrous sodium sulfate. The sample was then filtered, and the filtrate concentrated in vacuo. Gel Permeation Chromatography (chloroform) afforded 4,5-bis(benzothiophen-3-yl)-2-phenylthiazole (**S3**) as a white powder (0.59 g, 1.3 mmol, 65% yield). ^{1}H-NMR (300 MHz, $CDCl_3$, TMS, 25°C) δ (ppm) 7.42-7.50 (m, 7H), 7.81 (s, 2H), 7.86-8.18 (m 6H), HR-MS (MALDI-TOF): m/z calcd. for $C_{37}H_{23}NS_3$ $[M]^+$: 657.168; found 657.149.

4,5-Bis(2,5-diphenylthiazol-4-yl)-2-phenylthiazole (**2**): A two-necked flask was charged with 4,5-bis(benzothiophen-3-yl)-2-phenylthiazole (**S3**) (0.10 g, 0.23 mmol), bromobenzene (0.08 g, 0.51 mmol), di-*tert*-butylmethylphosphine tetrafluoroborate (0.011 g, 0.046 mmol), cesium carbonate (0.30 g, 0.92 mmol), palladium acetate (0.10 g, 0.046 mmol) and pivalic acid (0.011 g, 0.11 mmol) in mesitylene (2 mL). The mixture was heated under reflux at 150°C for 16 hours. Thereafter, it was filtered through celite, extracted with ethyl acetate, and the combined extracts were washed with water and dried over anhydrous sodium sulfate. Gel Permeation Chromatography (chloroform) afforded **2** (0.019 g, 0.032 mmol, 14% yield) as a colorless powder. ^{1}H-NMR (600 MHz, $CDCl_3$, TMS, 25°C) δ (ppm) 8.16 (d, J = 6.2 Hz, 2H), 7.60 (dd, J = 18.9, 7.9 Hz, 2H), 7.51 (dt, J = 18.6, 7.2 Hz, 3H), 7.33 (s, broad, 1H), 7.25 (s, 1H), 7.21-7.15 (m, 2H), 7.09 (m, 2H), 6.88 (d, J = 8.2 Hz, 2H), 6.84 (d, J = 8.2 Hz, 2H), 6.69 (s broad, 4H), 6.53 (s broad, 2H); ^{13}C NMR (151 MHz, CD_2Cl_2, TMS, 25°C) δ (ppm) 167.0, 149.0, 143.1, 139.8, 139.5, 139.1, 138.9, 134.1, 133.8, 133.3, 130.6, 129.4, 129.0, 128.2, 128.2, 128.0 - 127.6 (5 broad overlapping peaks observed), 126.7, 126.0, 124.7, 124.5, 124.3, 124.2, 124.0,

123.4, 122.2, 121.8, 121.5. HR-MS (ESI): m/z calcd. for $C_{37}H_{23}NS_3$: 577.0993 [M^+]; found: 577.0998.

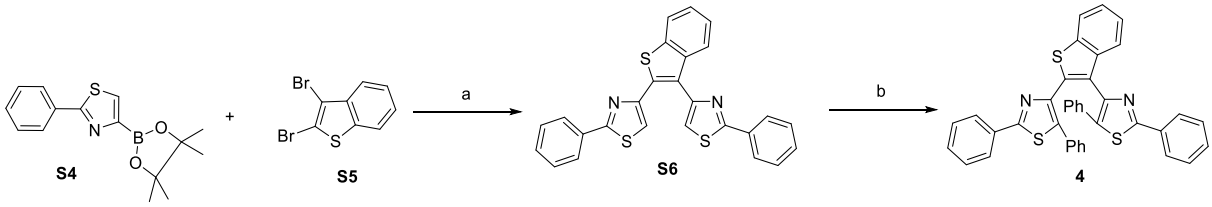

Scheme 2. *Synthesis of* ***4****: a) [Pd(PPh$_3$)$_4$], PPh$_3$, 2 M K$_3$PO$_4$, water/1,4-dioxane, THF 24 h, 110°C; b) Phenylboronic acid, (^{t}Bu)$_2$PMeHBF$_4$, pivalic acid, Cs$_2$CO$_3$, Pd(OAc)$_2$ 16 h, 150°C.*

4,4'-(benzo[b]thiophene-2,3-diyl)bis(2-phenylthiazole) (**S6**): A two-necked flask was charged with 2-phenyl-4-(4,4,5,5-tetramethyl-1,3,2-dioxaborolan-2-yl)thiazole (**S4**) (660 mg, 2.3 mmol), 2,3-dibromobenzo[b]thiophene (**S5**) (321 mg 1.1 mmol,), triphenylphosphine (43 mg, 0.165 mmol) and 2 M aqueous tripotassium phosphate (10 mL) in 1,4-dioxane (10 mL). After 60 minutes of stirring under nitrogen atmosphere, tetrakis(triphenylphosphine)palladium(0) (80 mg, 0.047 mmol) was added and stirred under nitrogen atmosphere at 110°C for 24 hours. The organic layer was then extracted with chloroform and the combined extracts were washed with water and dried over anhydrous sodium sulfate. The sample was then filtered, and the filtrate concentrated in vacuo. Gel Permeation Chromatography (chloroform) afforded 4,4'-(benzo[b]thiophene-2,3-diyl)bis(2-phenylthiazole) (**S6**) (0.35 g, 0.7 mmol, 70% yield) as a white powder. ^{1}H-

NMR (300 MHz, $CDCl_3$, TMS, 25°C) δ (ppm) 8.10-8.07 (m, 2H), 8.02-7.99 (m, 2H), 7.91-7.88 (m, 1H), 7.72-7.70 (m, 1H), 7.49-7.43 (m, 7H), 7.41-7.37 (m, 2H), 7.16 (s, 1H).

4,4'-(benzo[b]thiophene-2,3-diyl)bis(2,5-diphenylthiazole) (**4**): A two-necked flask was charged with 4,4'-(benzo[b]thiophene-2,3-diyl)bis(2-phenylthiazole) (**S7**) (0.20 g, 0.44 mmol), bromobenzene (0.16 g, 1.04 mmol), di-*tert*-butylmethylphosphine tetrafluoroborate (0.021 g, 0.09 mmol), cesium carbonate (0.054 g, 1.7 mmol), palladium acetate (0.019 mg, 85 μmol) and pivalic acid (0.026 g, 0.25 mmol) in mesitylene (1.5 mL). The mixture was heated under reflux at 150°C for 16 hours. Thereafter, it was filtered through celite, extracted with ethyl acetate and the combined extracts were washed with water and dried over anhydrous sodium sulfate. Gel Permeation Chromatography (chloroform) afforded **4** (0.050 g, 0.083 μmol, 16% yield) as a white powder. ^{1}H NMR (600 MHz, $CDCl_3$, TMS, 25°C) δ (ppm) 7.86 (d, J = 7.9 Hz, 1H), 7.80 (d, J = 7.9 Hz, 1H), 7,79 (m, 2H), 7.71 (dd, J = 7.9, 1.7 Hz, 2H), 7.41-7.33 (m, 8H), 7.07 (dd, J = 7.2 Hz, 1.4 Hz, 2H), 7.03 (t, J = 7.2 Hz, 2H), 7,00 (d, J = 7.8 Hz, 2H), 6.96-6.91 (m, 4H); ^{13}C NMR (151 MHz, $CDCl_3$, TMS, 25°C) δ (ppm) 165.0, 145.3, 143.8, 139.8, 136.2, 136.0, 135.8, 133.8, 133.4, 131.2, 130.5, 129.8, 129.6, 128.8, 128.7, 128.6 (2 overlapping peaks), 128.4, 128.4, 128.3, 128.1, 127.7, 126.5, 126.4, 124.9, 124.5, 122.0; HR-MS (ESI): m/z calcd. for $C_{38}H_{24}N_2S_3$: 604.1096 [M^+]; found: 604.1097.

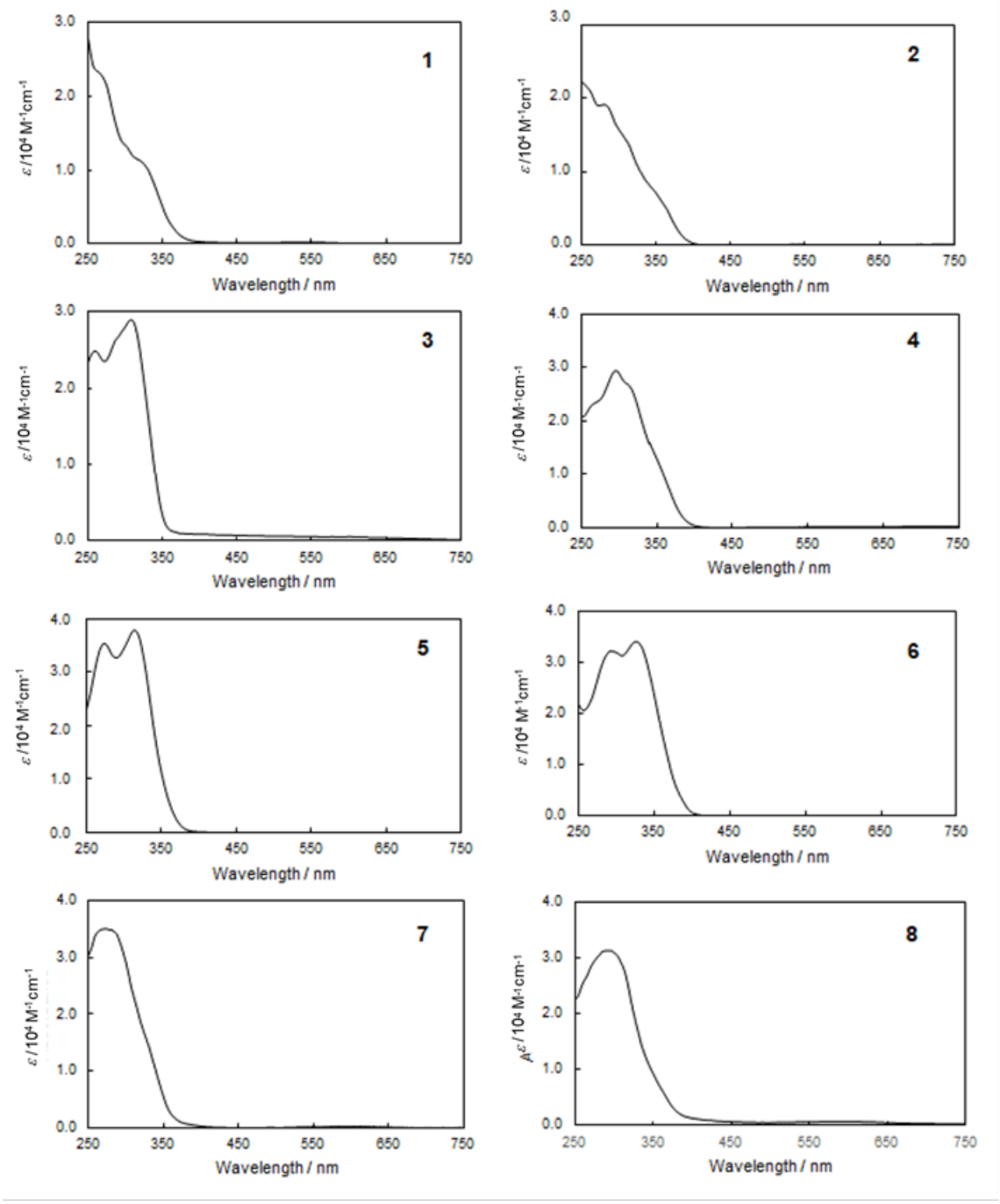

Figure S1. UV-vis spectra of compounds 1o-8o in acetonitrile.

Concentration = (1) 4.6×10^{-5} M; (2) 5.6×10^{-5} M; (3) 2.5×10^{-5} M; (4) 4.5×10^{-5} M; (5) 4.1×10^{-5} M; (6) 2.9×10^{-5} M; (7) 3.0×10^{-5} M; (8) 4.0×10^{-5} M.

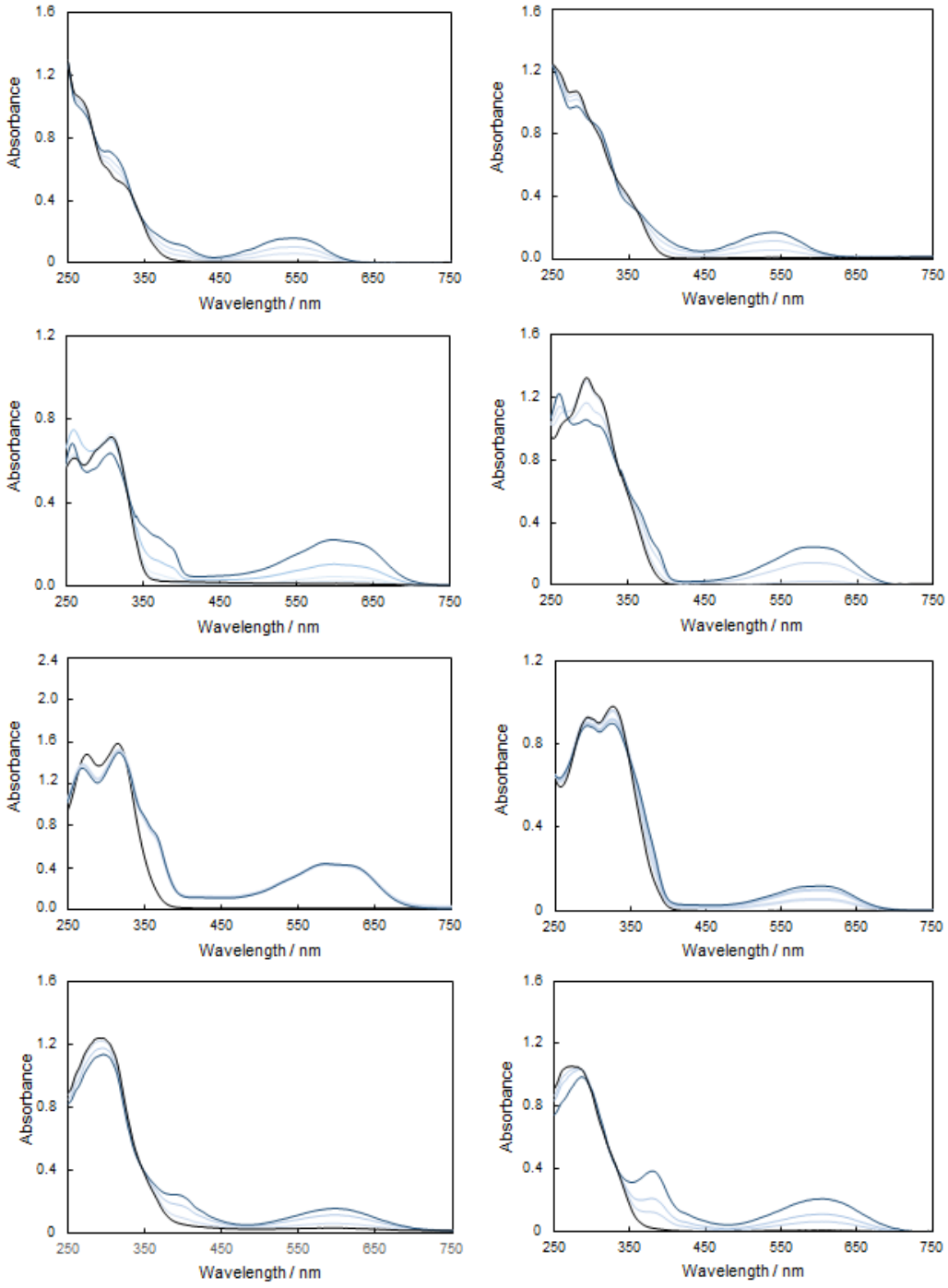

Figure S2. New absorption bands in the visible region upon irradiation of 1o–8o

in acetonitrile (UV light at 365 nm). Visible light irradiation turns them back to the o form. Initial concentration of o forms = (1) 4.6 × 10^{-5} M; (2) 5.6 × 10^{-5} M; (3) 2.5 × 10^{-5} M; (4) 4.5 × 10^{-5} M; (5) 4.1 × 10^{-5} M; (6) 2.9 × 10^{-5} M; (7) 3.0 × 10^{-5} M; (8) 4.0 × 10^{-5} M.

Table S1 Half-lifetime of c-form towards the non-photochemical cycloreversion reaction and the ratio of remaining species (T)

	k / s^{-1} [a]	$Ea_{c\text{-}o}$ /kJ mol^{-1} [b]	*A* / s^{-1} [b]
1	1.0 x 10^{-8}	127	1.4 x 10^{8}
2	5.1 x 10^{-8}	106	4.8 x 10^{11}
3[c]	2.9 x 10^{-10}	137	5.3 x 10^{15}
4	3.8 x 10^{-7}	114	2.5 x 10^{13}
5[d]	5.8 x 10^{-4}	112	5.2 x 10^{16}
6[d]	4.9 x 10^{-3}	104	1.7 x 10^{26}
7	6.5 x 10^{-7}	92	1.6 x 10^{10}
8	1.2 x 10^{-2}	37	4.3 x 10^{4}

All measurements reported in toluene. [a] rate constant of a first-order decay at 20°C; [b] the parameters of thermal cycloreversion reaction by means of Arrhenius relationship of temperature-dependent cycloreversion kinetics following Arrhenius's equation: $\ln k = \ln A - \frac{Ea}{RT}$; [c] data from Ref.2; [d] data from Ref.3.

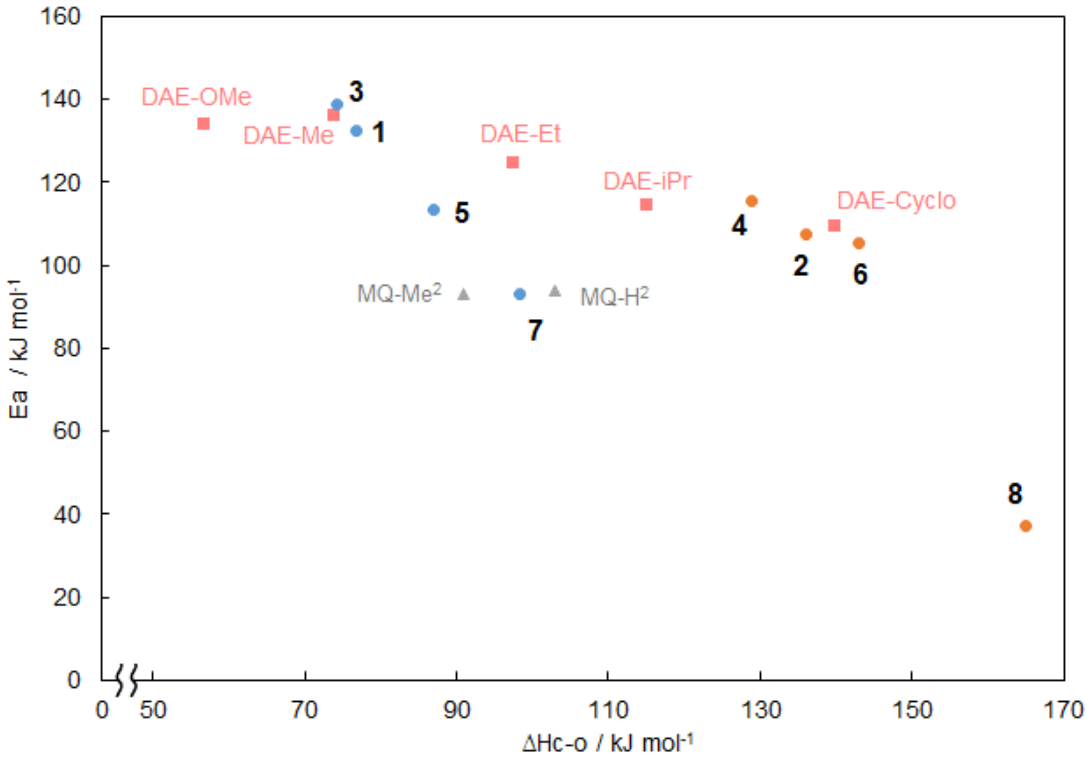

Figure S3 The plots of activation energy vs $\Delta H_{c\text{-}o}$ for terarylenes and diarylethenes. The molecular structures of the diarylethene references are also described. Their corresponding ΔH_{iso} have been calculated by the same method as shown table 2

using the B3LYP functional with the 6-31G(d) basis set. The reference data are from the literature.[4-7]

a)

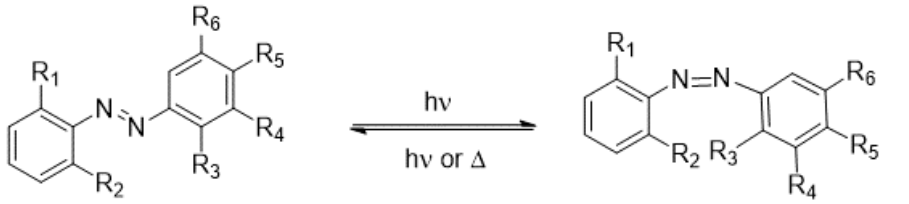

(E)-azobenzene derivatives (Z)-azobenzene derivatives

	R_1	**R_2**	**R_3**	**R_4**	**R_5**	**R_6**
Azo-H	H	H	H	H	H	H
Azo-Me	H	H	H	H	Me	H
Azo-Cl	H	H	H	H	Cl	H
Azo-NO_2	H	H	H	NO_2	H	H
Azo$(Me)_2$	Me	H	Me	H	H	H
Azo$(Me)_2$-NO_2	Me	H	Me	H	H	NO_2
Azo(Me)	Me	H	H	H	H	H
Azo$(Me)_3$	Me	Me	Me	H	H	H

b)

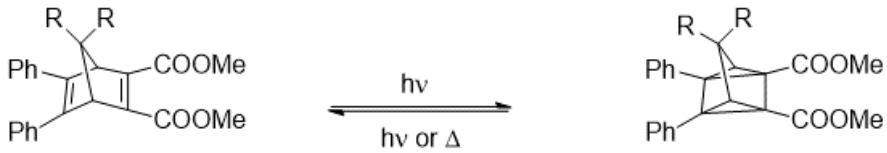

Norbornadiene derivatives (NBD-R_2) Quadricyclane

	R
NBD-H_2	H
NBD-Me_2	Me
NBD-iPr_2	isopropyl
NBD-tBu$_2$	*tert*-butyl

c)

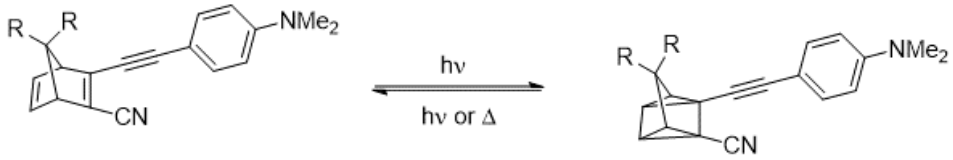

MQ-R_2

	R
MQ-H_2	H
MQ-Me_2	H

d)

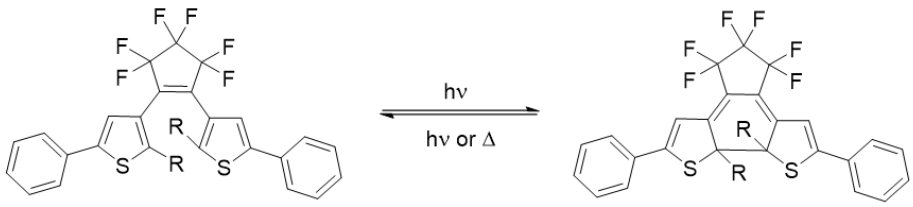

	R
DAE-OMe	Methoxy
DAE-Me	Me
DAE-Et	Ethyl
DAE-iPr	isopropyl
DAE-Cyclo	Cyclohexyl

Figure S4 The molecular structures of referenced data.

a) azobenzene derivatives,[4] b) Norbornadiene derivatives,[5] c) MQ-R2 series,[5] d) Diarylethene derivatives.[6,7]

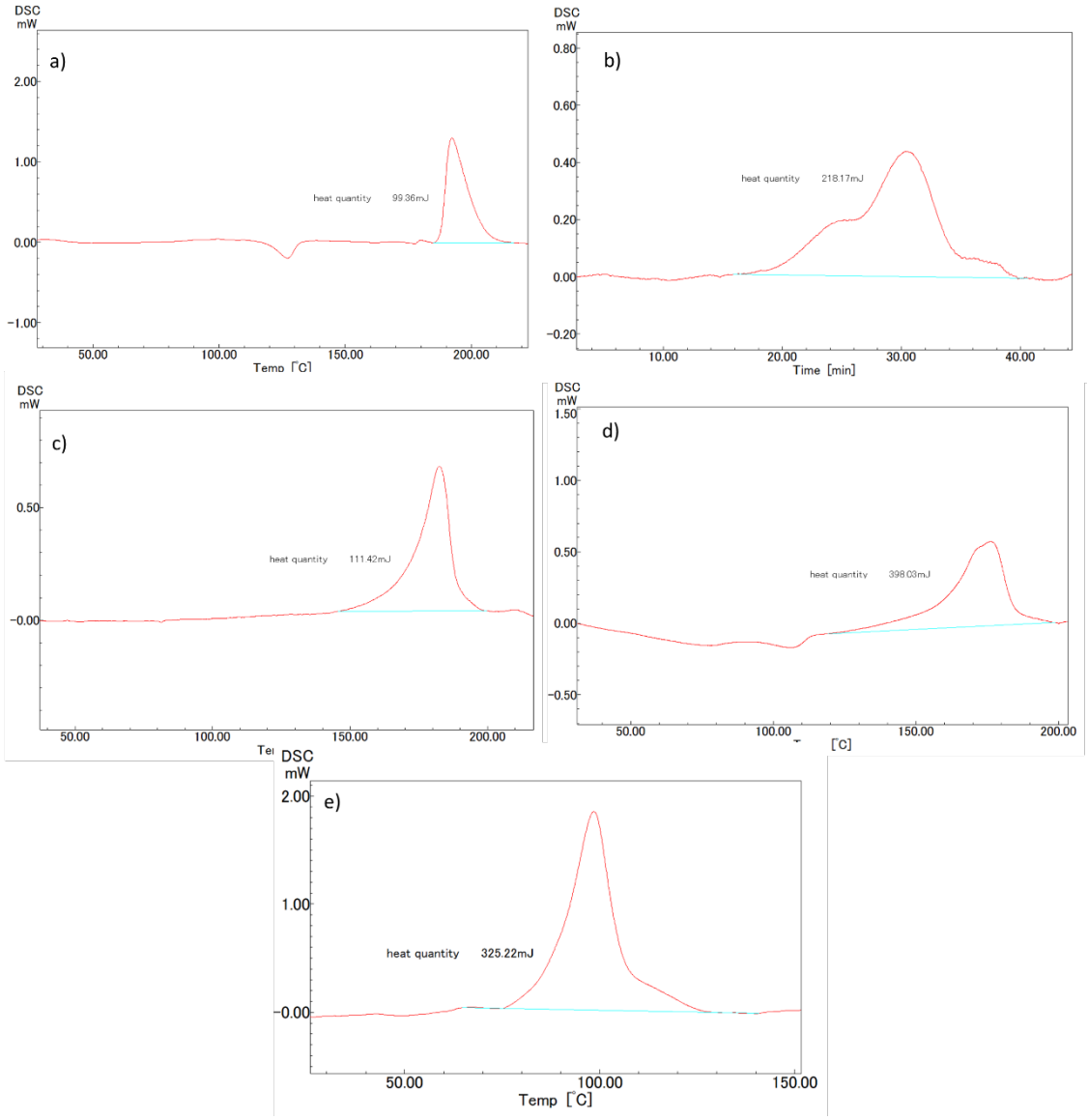

Figure S5. DSC scanning spectra of compounds 1-4 and 7. The heat quantity of the powder containing a photostationary state mixture for compounds 1 (a), 2 (b), 3 (c), 4 (d) and 7 (e) were measured. The scan speed and the packed weight of powder in the DSC holder are a) 5°C min^{-1} and 4.0 mg, b) 5°C min^{-1} and 2.4 mg, c) 8°C min^{-1} and 2.5 mg, d) 5°C min^{-1} and 3.1 mg, e) 5°C min^{-1} and 3.2 mg.

Table S2 Summary of DSC measurements

	Heat quantity[a] (mJ g^{-1})	Conversion rate of **c**-form[b]	$\Delta H_{c\text{-}o,\text{measured}}$[c] (kJ mol^{-1})
1	41.4	0.58	32.7
2	87.3	0.45	114
3	35.9	0.70	24.8
4	124	0.69	109.6
7	81.3	0.62	70.6

[a] data are estimated by the integration for the peak of heat release in DSC measurement with a mass of each compound. [b] data are estimated using UV-vis spectrum by comparing the **o**/**c** form of mixture powder dissolved in acetonitrile and the **o**-form induced by irradiation of visible light. [c] data are estimated with conversion rate of **c**-form.

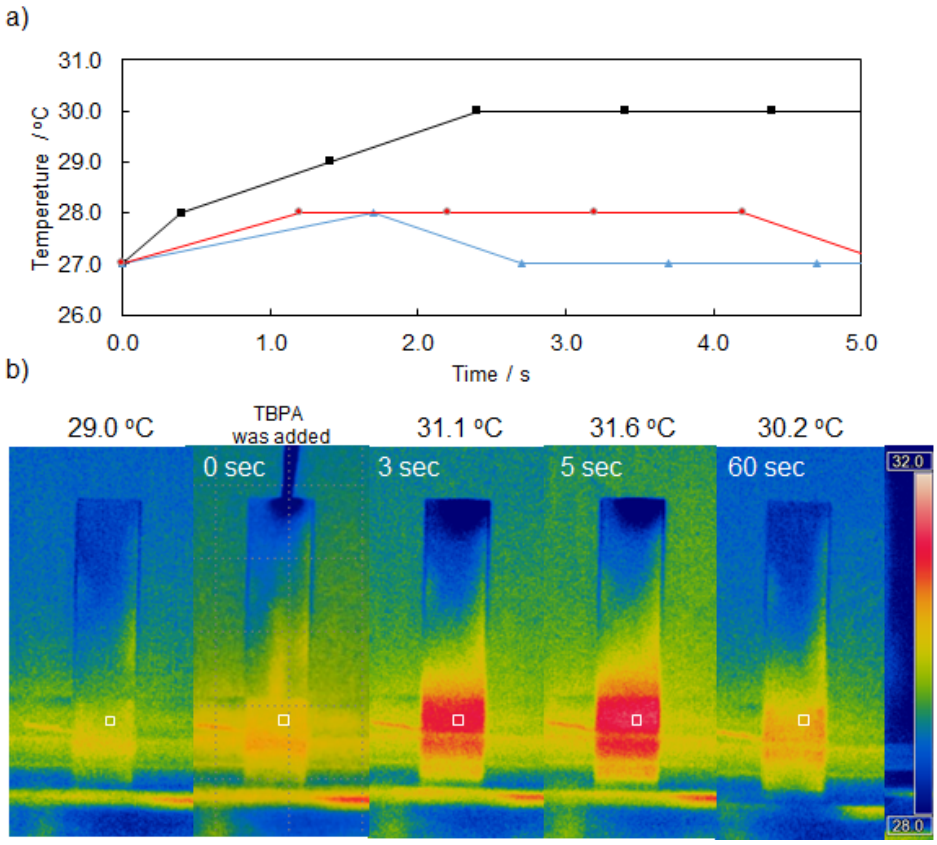

Figure S6. a) Temperature increase after adding 5 mol% of TBPA in acetonitrile (0.05 mL) into 1 mL of chloroform solution of 7c/o (black), 7o (red), and only chloroform (blue). Concentration of c-form = 5.0 x 10^{-2} M. The temperature was monitored by a sheathed

thermocouple. b) Thermographic images after adding 5 mol% of TBPA in acetonitrile (0.05 mL) into chloroform (1 mL) in a quartz cell.

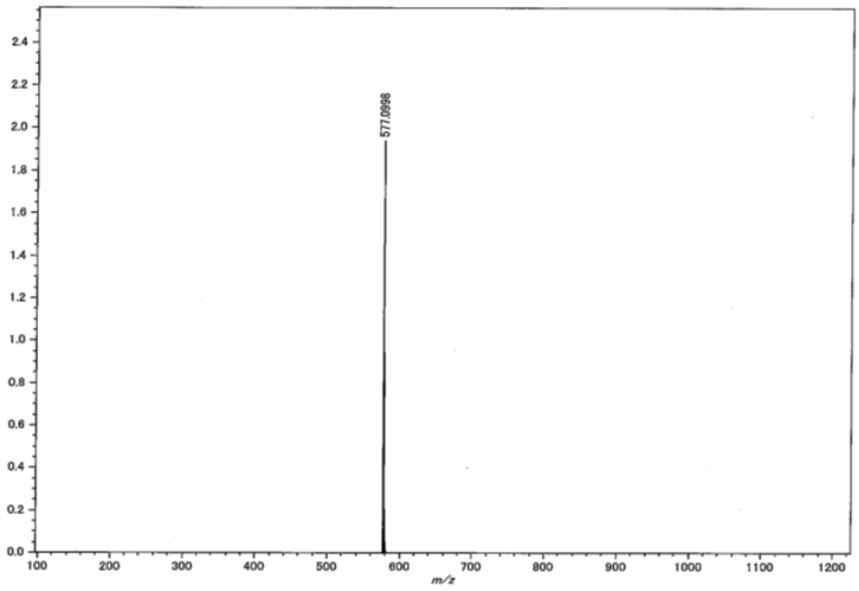

Figure S7 HR-MS data of 2o (MALDI-TOF).

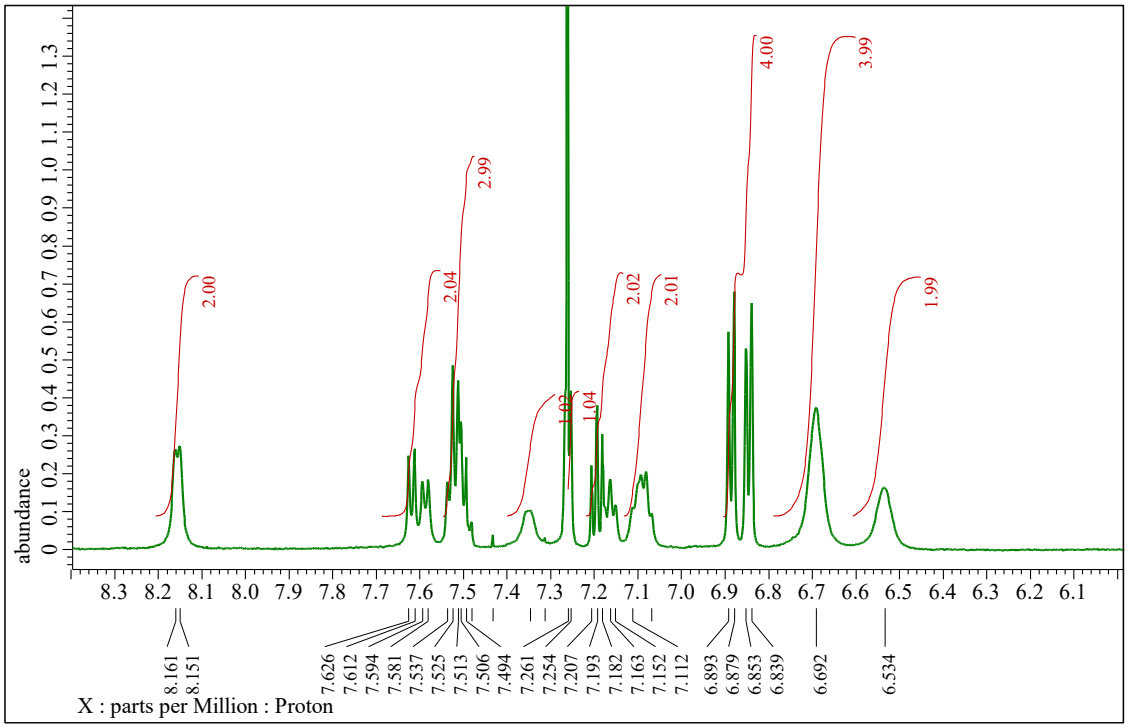

Figure S8. ^{1}H NMR spectrum of 2o (600 MHz, $CDCl_3$, TMS, 25°C).

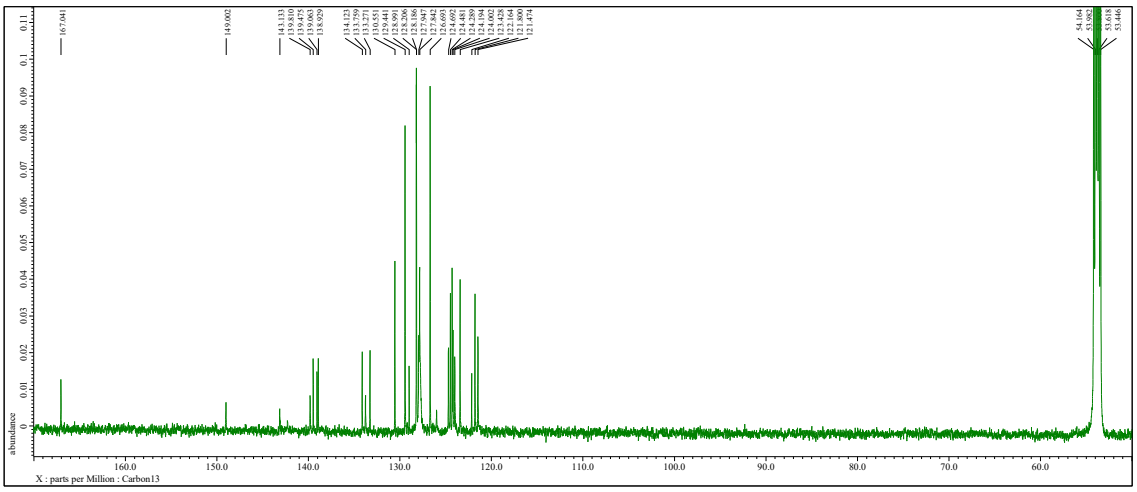

Figure S9 ^{13}C NMR spectrum of 2o (151 MHz, CD_2Cl_2, TMS, 25°C).

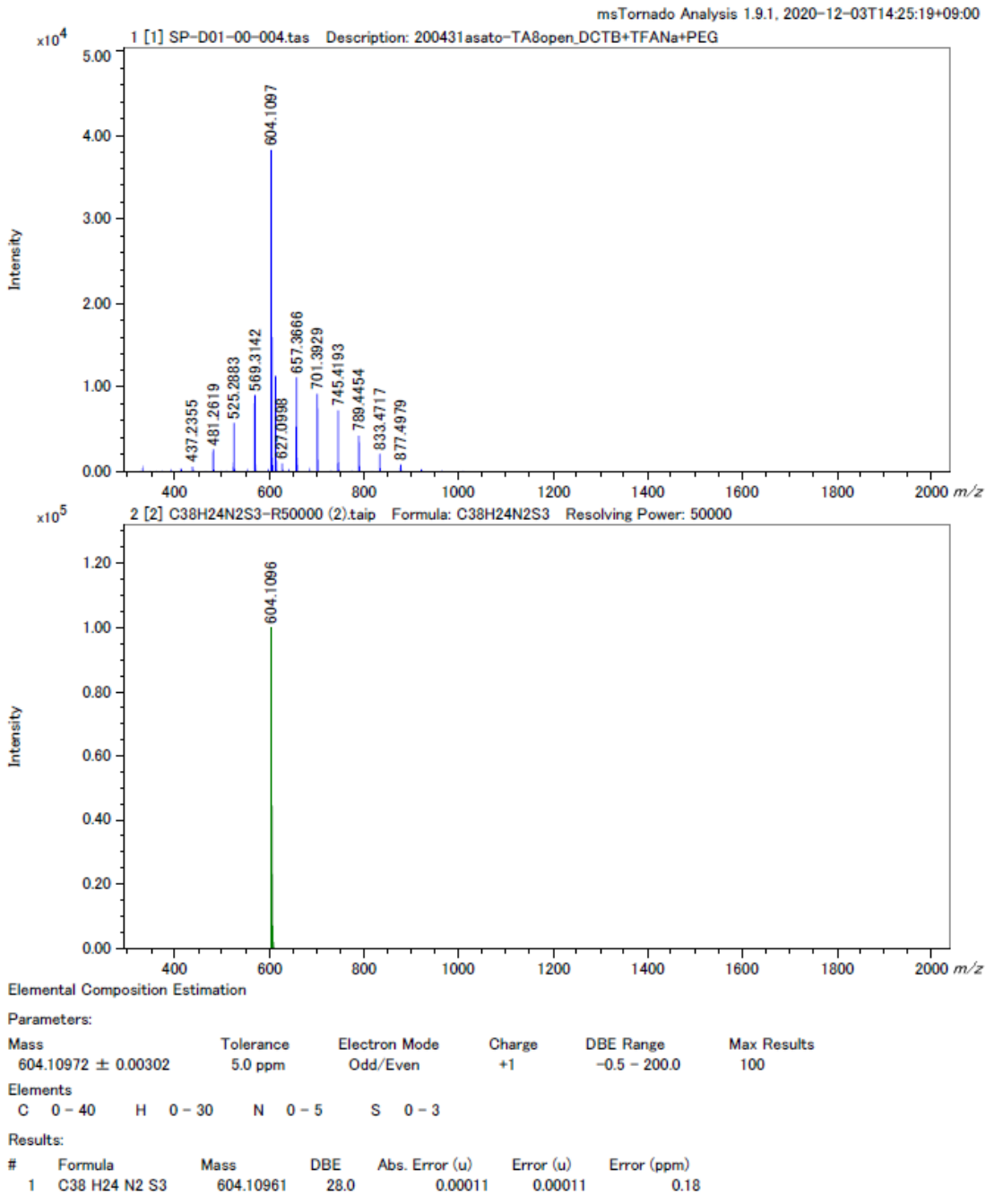

Figure S10 HR-MS data measurement (Top) and calculation result (bottom) of 4o. MALDI-Spiral-TOF system with polyethylene glycol as internal standard.

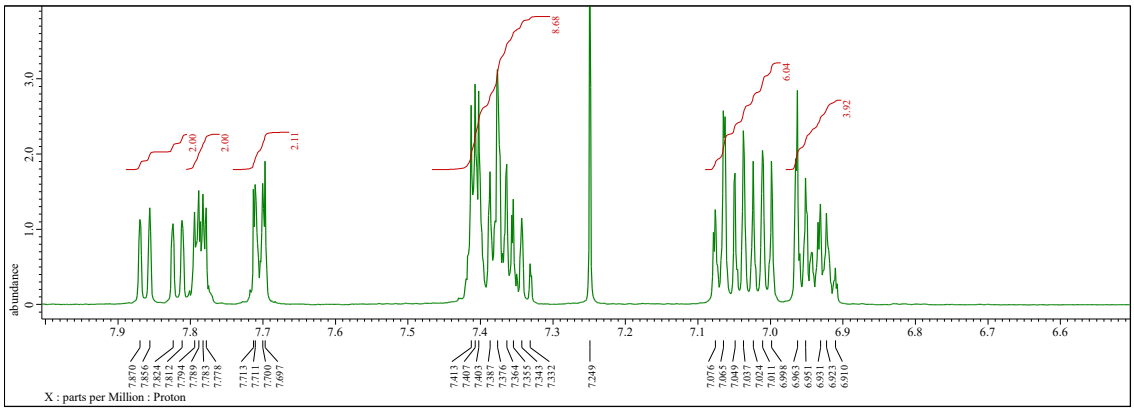

Figure S11 ^{1}H-NMR spectrum of 4o (600 MHz, $CDCl_3$, TMS, 25°C).

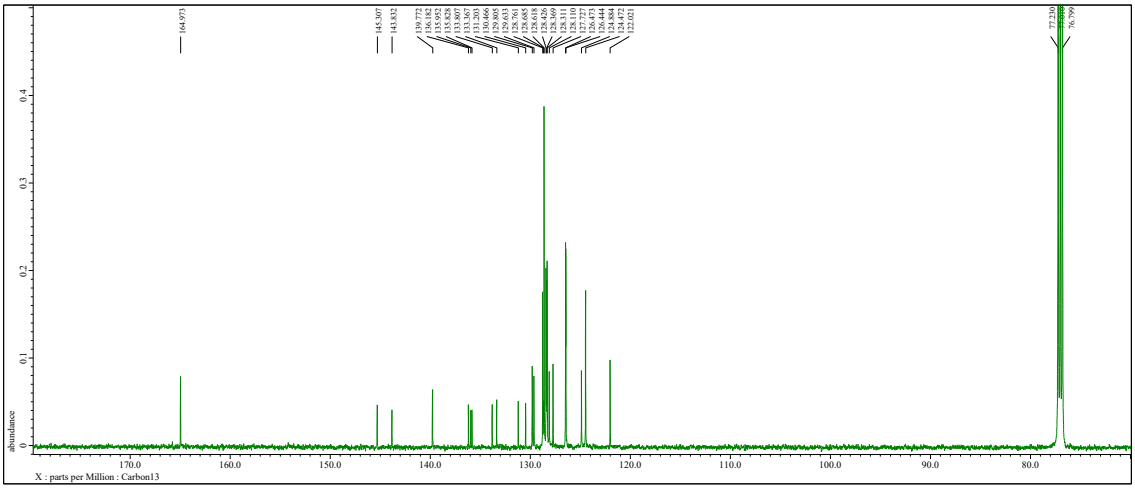

Figure S12. ^{13}C NMR spectrum of **4o** (151 MHz, $CDCl_3$, TMS, 25°C).

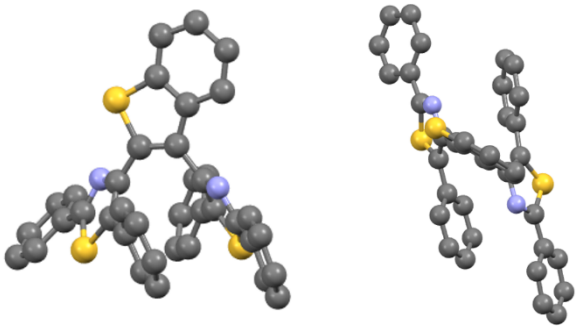

Figure S13. X-ray Structure of **4o**. Gray: carbon, yellow: sulfur, blue: nitrogen.

References

[1] Frisch, M. J.; Trucks, G.W.; Schlegel, H. B.; Scuseria, G. E.; Robb, M. A.; Cheeseman, J. R.; Scalmani, G.; Barone, V.; Mennucci, B.; Petersson, G. A.; Nakatsuji, H.; Caricato, M.; Li, X.; Hratchian, H. P.; Izmaylov, A. F.; Bloino, J.; Zheng, G.; Sonnenberg, J. L.; Hada, M.; Ehara, M.; Toyota, K.; Fukuda, R.; Hasegawa, J.; Ishida, M.; Nakajima, T.; Honda, Y.; Kitao, O.; Nakai, H.; Vreven, T.; Montgomery Jr, J. A.; Peralta, J. E.; Ogliaro, F.; Bearpark, M.; Heyd, J. J.; Brothers, E.; Kudin, K. N.; Staroverov, V. N.; Kobayashi, R.; Normand, J.; Raghavachari, K.; Rendell, A.; Burant, J. C.; Iyengar, S. S.; Tomasi, J.; Cossi, M.; Rega, N.; Millam, J. M.; Klene, M.; Knox, J. E.; Cross, J. B.; Bakken, V.; Adamo, C.; Jaramillo, J.; Gomperts, R.; Stratmann, R. E.; Yazyev, O.; Austin, A. J.; Cammi, R.; Pomelli, C.; Ochterski, J. W.; Martin, R. L.; Morokuma, K.; Zakrzewski, V. G.; Voth, G. A.; Salvador, P.; Dannenberg, J. J.; Dapprich, S.; Daniels, A. D.; Farkas, Ö.; Foresman, J. B.; Ortiz, J. V.; Cioslowski, J.; Fox, D. J. Gaussian 09 Revision A.02, Gaussian Inc. Wallingford CT, 2009.

[2] Kucharski, T. J.; Tian, Y.; Akbulatov, S.; Boulatov, R. *Sci. Review*. **4,** 4449 (2011).

[3] Jorner, K. et al. *J. Mater. Chem. A*. **5,** 12369-12378 (2017).

[4] Shoji, H.; Kitagawa, D.; Kobatake, S. *New J. Chem.* **38,** 933 (2014).

[5] Morimitsu, K.; Shibata, K.; Kobatake, S.; Irie, M. *Chem. Lett*. **31,** 6, 572-573 (2002).